JOURNAL OF MATERIALS SCIENCE: MATERIALS IN ELECTRONICS **16** (2005) 633–643

REVIEW
Optical nonlinearity in photonic glasses

KEIJI TANAKA
Department of Applied Physics, Graduate School of Engineering, Hokkaido University, Kita-ku, Sapporo 060-8628, Japan
E-mail: keiji@eng.hokudai.ac.jp

A brief review on optical nonlinearity in photonic glasses is given. For the third-order, relationship between two-photon absorption and nonlinear refractive-index is considered using a formalism developed for crystalline semiconductors. Stimulated light scattering and super-continuum generation in optical fibers are also introduced. Prominent resonant-type nonlinearity in particle-embedded glasses is described. For the second-order, a variety of poling methods are summarized. Finally, it is pointed out that different photoinduced changes can appear when excited by linear and nonlinear optical processes, and the feature is related with glass structures. © *2005 Springer Science + Business Media, Inc.*

1. Introduction

With developments of optical fibers and pulsed lasers, the optical nonlinearity in photonic glasses evokes increasing interest [1–3]. The third-order polarization provides several nonlinear phenomena such as intensity-dependent absorption and intensity-dependent refractive-index, which can be utilized as power stabilizers, all-optical switches, and so forth. By contrast, in high-power glass lasers, self-focusing effects arising from intensity-dependent refractive-index increases pose serious problems. On the other hand, the second-order polarization, which appears in poled glasses, can be utilized in second-harmonic generators. The present article provides a brief overall review on the optical nonlinearity in *inorganic* glasses. Here, it should be mentioned that, in many respects, organic polymers exhibit similar features to those of the glass, as listed in recent books by Sutherland [4] and Boyd [5]. In general, the glass is more stable, while the polymer could give greater nonlinearity, so that the two will be competitive in practical applications.

The glass is also competitive with crystals. A great advantage of the glass is structural controllability in three scales. First, the atomic composition can be continuously tailored [6]. For instance, a nonlinear optical glass which has any refractive index in a range of 1.4–3.2 at wavelength of $\sim$1 μm is available. Second, the atomic structure can be modified more-or-less easily using, e.g., light beams, with minimal scales of submicron meter. Such modifications may be regarded as photoinduced phenomena, which can be employed for adding second-order nonlinearity to selected regions. Lastly, macroscopic shapes can be changed to arbitrary bulk forms, fibers, thin layers, and micro-particles [7, 8].

Here, fiber and film waveguides may be the most important for nonlinear applications with the two reasons. One is light power density can be increased by reducing the lateral size, i.e. film thickness or fiber diameter, to sub-micron meter scales [9–11]. The other is, in specific, the fiber can provide long lengths for light-glass interaction, which are not limited by diffraction [1]. These scale factors provide apparent enhancements of nonlinear effects in glasses, provided that intrinsic nonlinearity may be smaller than that in crystals.

Before proceeding further, it would be appropriate to introduce a nonlinear formula [4, 5]. For simplicity, we take the polarization P and the electric field E to be scalar quantities. Then, very simply, P can be written down in the CGS unit as;

$$P = \chi^{(1)}E + \chi^{(2)}EE + \chi^{(3)}EEE + \cdots, \qquad (1)$$

where the first term $\chi^{(1)}E$ depicts the conventional linear response, and $\chi^{(2)}$ and $\chi^{(3)}$ represent the second- and the third-order nonlinear susceptibility. As is known, $\chi^{(1)}$ is related with the linear refractive-index n_0 as $n_0 = \{1 + 4\pi\chi^{(1)}\}^{1/2}$. On the other hand, the second term provides such time dependence as $\sin\{(\omega \pm \omega)t\}$, so that it could produce dc and second-overtone (2ω) signals. In a similar way, the third could modify the fundamental (ω) signal and generate a third-overtone (3ω). Nevertheless, since a refractive index changes with frequency, it is difficult in the over-tone generations to satisfy the so-called phase-matching condition [4, 5], e.g. $\varphi_{3\omega} = 3\varphi_{\omega}$, where φ is the phase of electric fields in glasses [12]. Therefore, the fundamental-signal processing may be the most important. Microscopically, the nonlinear terms arise through several mechanisms such as electronic, atomic (including molecular motions), electrostatic, and thermal processes. Among these, the electronic process can provide the fastest response with fs – ps time scales, which will be needed for optical information technologies. Accordingly, we will focus on the process hereafter, which is sectioned as follows.

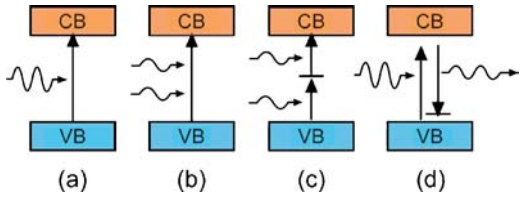

Figure 1 Schematic illustrations of (a) one-photon absorption, (b) two-photon absorption, (c) two-step absorption via a midgap state, and (d) Raman-scattering process in a semiconductor with a valence (VB) and a conduction band (CB).

In Section 2, we will treat conventional homogeneous glasses. These are optically isotropic, and accordingly, $\chi^{(2)} = 0$, because the isotropic disordered structure appears to be centro-symmetric. Then, the lowest nonlinear term becomes to be $\chi^{(3)}EEE$. When $\chi^{(3)}EEE$ can be written as $\chi^{(3)}IE$, where I is the light intensity, we can define an effective refractive-index n as $n = n_0 + n_2 I$, where n_2 is sometimes called the second-order index of refraction [5]. As is known, in nonlinear optics, the notation poses complicated problems due to several definitions of physical quantities. Then, a conversion $n_2\,(\mathrm{cm}^2/\mathrm{W}) \approx 0.04\chi^{(3)}\,(\mathrm{esu})/n_0^2$ may be frequently employed [5]. On the other hand, for light absorption, which is proportional to $\langle E\mathrm{d}P/\mathrm{d}t\rangle$, where $\langle\ \rangle$ represents a time average, we should take imaginary parts of $\chi^{(1)}$ and $\chi^{(3)}$ into account, which cause one- and two-photon absorption (see, Fig. 1). In such cases, an effective absorption coefficient can be written down as $\alpha(\mathrm{cm}^{-1}) + \beta(\mathrm{cm/W})I(\mathrm{W/cm}^2)$. n_2 and β will be connected through nonlinear Kramers-Krőnig relations (see, Equations 6 and 8).

Section 3 will focus upon non-centro-symmetry. It has been discovered since the middle of '80s that several kinds of poling treatments can add $\chi^{(2)}$ to glasses [13]. For instance, Österberg and Margulis [14] demonstrated intense second-harmonic generation in laser-irradiated glass fibers. Such work began with silica, and it has been directed to more complicated glasses. Magnitudes of $\chi^{(2)}$ may be smaller than those in crystals due to disordered atomic structures in glasses, while the structural controllability could offer some advantages.

Section 4 introduces the glass which incorporates fine semiconductor and metal particles. Such nanostructured glasses are known to exhibit large optical nonlinearity [4, 5, 15]. However, as will be described, the overall feature remains to be studied.

In Section 5, we will consider photoinduced phenomena. Intense light, which is needed for providing optical nonlinearity, is likely to modify glass structures. Actually, fiber Bragg gratings [1, 16] have already been commercially produced using excimer lasers, in which roles of nonlinear optical excitation may be important. Three-dimensional refractive-index modifications can also be produced by controlling light focusing [17]. If the light is more intense, it may give some damage, which is promising for fabrications of three-dimensional interconnected hollow structures [18, 19].

Section 6 will give a summary.

2. Third-order nonlinearity in homogeneous glass

2.1. Experimental

Substantial data are available for n_2 at transparent wavelengths [4]. However, to the author's knowledge, all experiments utilize lasers, and no spectral dependence has been reported. Since the dispersion of n_2 at transparent regions is relatively small (see, Fig. 5), detailed spectral measurements may not necessarily be required. In addition, we should also note that, in comparison with n_0 measurements, n_2 evaluations are much more difficult [4]. The biggest difficulty, which is common to all nonlinear experiments, is the light intensity. Normally, light is pulsed and focussed, in which temporal and spatial profiles are not simple, so that intensity evaluations cannot be straightforward. For instance, if the profile be Gaussian, can we simply take the peak value for nonlinearity evaluations? With such measuring difficulties and also with some specific problems inherent to glasses, even for a reference glass SiO_2, reported n_2 values vary at 1–3 $\times\ 10^{-20}$ m^2/W [4]. In other glasses, different values of a factor of ~10 are reported [4, 9, 15, 17, 20].

However, we see in Table I a general tendency for n_2. Halide glasses (BeF_2) have the smallest, light-metal oxides (BK-7) and SiO_2 give similar values, heavy-metal oxides such as PbO-SiO_2 (SF-59) are the next, and the largest is obtained in chalcogenide glasses (As_2S_3) [4, 9, 15, 17, 20–25]. The largest value reported so far may be $n_2 = 8 \times 10^{-12}$ cm^2/W in $Ag_{20}As_{32}Se_{48}$ at wavelength of 1.05 μm [26], which is $\sim 10^4$ times as large as that of SiO_2. For temperature dependence, it is reported that $\mathrm{d}n_2/\mathrm{d}T < 0$ in a silica fiber [27].

Fig. 2 summarizes β spectra for SiO_2, As_2S_3, and two PbO-SiO_2 glasses [28]. Bi_2O_3-B_2O_3 glasses [29] exhibit similar features to those of the lead glass [30]. We see that all the β spectra seem to have maxima at midgap regions, $\hbar\omega \approx E_g/2$. However, this is not

TABLE I Linear (E_g, n_0, α_0) and nonlinear (n_2, β, β_{max}) optical properties and figure-of-merits ($2\beta\lambda_0/n_2$, n_2/α_0) in some glasses. E_g is an optical bandgap energy [17], n_0 the refractive index [17], α_0 the attenuation coefficient [28], n_2 the intensity-dependent refractive-index [4, 5, 17], β the two-photon absorption coefficient [28], and β_{max} the maximal value. Except E_g and β_{max}, the values are evaluated at optical communication wavelengths of 1–1.5 μm. BK-7 is a borosilicate glass and SF-59 represents data for lead-silicate glasses with ~57 mol.% PbO

Glass	E_g (eV)	n_0	α_0 (cm^{-1})	n_2 ($\times 10^{-16}$ cm^2/W)	β (cm/GW)	β_{max} (cm/GW)	$2\beta\lambda_0/n_2$	n_2/α_0 (cm^3/GW)
SiO_2	10	1.5	10^{-6}	2	$<10^{-2}$	1	<10	0.2
BK-7	4	1.5		3				
SF-59	3.8	2.0		30	$<10^{-1}$	10		
As_2S_3	2.4	2.5	10^{-3}	200	10^{-2}	50	0.1	0.02
BeF_2	10	1.3		0.8				

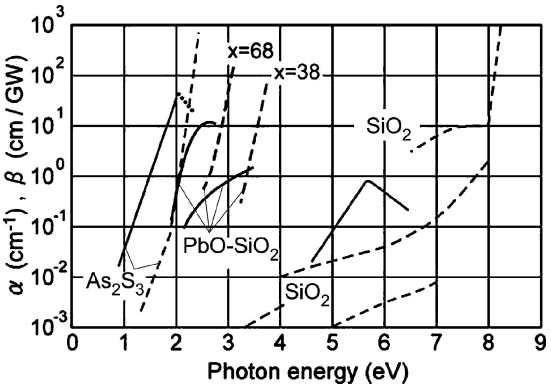

Figure 2 One- (dashed line) and two-photon (solid line) absorption spectra, α and β, in SiO_2 [35, 36], 38PbO-62SiO_2, 68PbO-32SiO_2 [30], and As_2S_3 [31]. For SiO_2, α at transparent regions ($\hbar\omega \leq 8.0$ eV) should be regarded as attenuation coefficients, which are not reproducible, probably due to impurities, defects, and light scattering. The dotted line for As_2S_3 at $\hbar\omega \geq 2.0$ eV indicates two-step absorption.

conclusive, since As_2S_3 at$\hbar\omega \geq 2.0$ eV possesses two-step absorption (see, Fig. 1), which masks two-photon signals [31]. We also see that the maximal β ($\sim 10^0$ cm/GW) in SiO_2 is substantially smaller than those in the others. Note that such a marked difference does not exist in maximal α, which is commonly $\sim 10^6$ cm^{-1} at super-bandgap regions in SiO_2 and As_2S_3 [32]. It may be valuable to mention here that, in some glasses, two-photon excitation produces appreciable photocurrents [33, 34].

2.2. Theoretical

For $\chi^{(3)}$, theoretical treatments of glass, liquid, and crystal could be principally the same. The glass and the liquid can be treated similarly in a sense that the both are optically isotropic. Hence, many ideas stemming from kinds of *chemical-bond pictures* have been proposed [5]. On the other hand, the magnitude of $\chi^{(3)}$ in glasses appears to be similar to that in the corresponding crystals, since electronic structures are governed by short-range atomic structures within $\sim$0.5 nm [6], which is much shorter than the wavelength ($\sim$500 nm) of visible light. Specifically, since n_2 is governed by integrated electronic absorption (see, Equation 8), the magnitudes become to be roughly the same in glass and crystal. For instance, in crystalline and glassy SiO_2 at near infrared wavelength, the difference in n_2 seems to be comparable with experimental accuracy; i.e. in crystalline and glassy SiO_2, $\chi^{(3)} \approx 1.14 \times 10^{-13}$ esu and 0.85×10^{-13} esu [4]. Then, using formula derived for semiconductor crystals, we can apply a kind of *band pictures* to glasses [28], as described below.

2.2.1. Estimation of nonlinear refractivity

Several semi-empirical relationships have been proposed for $\chi^{(3)}$ or n_2 [5]. Such relations are useful, since measurements of nonlinear optical constants are much more difficult than those of linear constants, as mentioned earlier. Naturally, a simpler relation is less accurate. The simplest may be the one given by Wang, $\chi^{(3)} \propto \{\chi^{(1)}\}^4$, which can be regarded as a generalized Miller's rule [5]. Boling *et al.* [37] have derived several relations, in which the simplest may be;

$$n_2\,(10^{-13}\,\text{esu}) \approx 391\,(n_\text{d} - 1)/\nu_\text{d}^{5/4}, \qquad (2)$$

where n_d is the refractive index at the *d*-line ($\lambda = 588$ nm) and ν_d is the Abbe number. This relation contains only these two linear macroscopic parameters, which can be evaluated easily, and accordingly, it has been frequently utilized for estimations of n_2. It actually provides a good approximation for small n_d glasses with $n_\text{d} \leq 1.7$ [5, 37]. For high n_d glasses, Lines [20] has proposed a relation, which contains also the atomic distance, and others derive more complicated formula [38, 39]. Ab initio calculations for TeO_2-based glasses have also been reported recently [40]. However, these relations can hardly predict wavelength dependence. That is, the estimated n_2 may be regarded as long-wavelength limit values (see, Fig. 5). In addition, the material is assumed to be transparent, so that relations between n_2 and β cannot be known at all.

Nonlinear optical properties of semiconductor crystals have been studied more-or-less deeply [5], and applications of the concept to glasses appear to be tempting. Tanaka [28] has adopted a band picture, which is developed by Sheik-Bahae *et al.* [41], to some glasses. Their result gives a universal relationship;

$$n_2 = KG(\hbar\omega/E_\text{g})\big/\left(n_0 E_\text{g}^4\right), \qquad (3)$$

for crystals with energy gaps of 1–10 eV, where K is a fixed constant and $G(\hbar\omega/E_\text{g})$ is a spectral function, where E_g is the bandgap energy. For E_g in glasses, we may take the so-called Tauc gap [6] if it is known, or otherwise, the photon energy $\hbar\omega$ at $\alpha \approx 10^3$ cm^{-1}. As shown in Fig. 3, the universal line gives reasonable

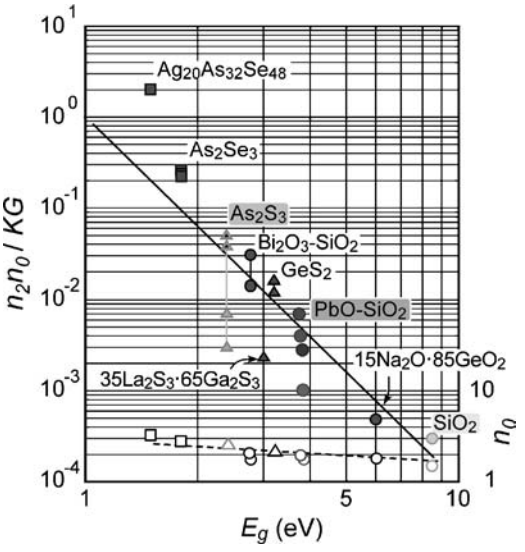

Figure 3 The Sheik-Bahaes' relation $n_2 n_0 = KG(\hbar\omega/E_\text{g})/E_\text{g}^4$ (solid line), related data (solid symbols), the Moss rule $n_0^4 E_\text{g} = 77$ (dashed line), and related data (open symbols) for the oxide (circles), sulfide (triangles), and selenide (squares). The four data for As_2S_3 are obtained from different publications, while those for PbO-SiO_2 with slightly different E_g correspond to different compositions. The illustration is modified to the previous [28] with additions of $Ag_{20}As_{32}Se_{48}$ [26], Bi_2O_3-silica glasses [43], $35La_2S_3$-$65Ga_2S_3$ [44], and $15Na_2O$-$85GeO_2$ [45].

agreements with published data for glasses, while the agreement is not so satisfactory as in the case for crystals [41]. The worse agreement in the glasses may be partly due to experimental difficulties including quasi-stable glass properties. In addition, band-tail states, which are not taken into account in Equation 3, may cause larger deviations in smaller bandgap glasses such as $Ag_{20}As_{32}Se_{48}$. Incidentally, as shown by a dashed line in Fig. 3, the Moss rule $n_0^4 E_g = 77$ [42], which has been proposed for crystalline semiconductors, gives satisfactory fits also for glasses.

2.2.2. Non-linear Kramers-Krőnig relationship

To obtain unified insights into the third-order optical nonlinearity, n_2 and β, we can take another approach. Here, we start with the absorption, and then calculate the refractive index using Kramers-Krőnig relationships. As illustrated in Fig. 4, this approach is able to provide unified understandings of atomic structures and optical properties, since the absorption spectra can be related with electronic structures more directly. The method is recently demonstrated to be useful for understanding high optical nonlinearity in PbO-SiO_2 glasses [46].

As is known, $\alpha(\hbar\omega)$ and $\beta(\hbar\omega)$ can be written for glasses, neglecting momentum conservation rules, as [28];

$$\alpha(\hbar\omega) \propto |\langle\varphi_f|H|\varphi_i\rangle|^2 \int D_f(E+\hbar\omega)D_i(E)\,\mathrm{d}E, \quad (4)$$

$$\beta(\hbar\omega) \propto |\Sigma_n \langle\varphi_f|H|\varphi_n\rangle\langle\varphi_n|H|\varphi_i\rangle/(E_{ni}-\hbar\omega)|^2 \times \int D_f(E+2\hbar\omega)D_i(E)\,\mathrm{d}E, \quad (5)$$

where H is the perturbation Hamiltonian, φ is a related electron wavefunction, and D is a density-of-states, in which the subscripts i, n, and f represent initial, intermediate, and final states. Here, the energy dependence of the wavefunctions is neglected for simplicity. These equations show that α and β are connected to the electronic structure, i.e. wavefunctions and densities-of-states, which is determined by atom species and bonding structures [6].

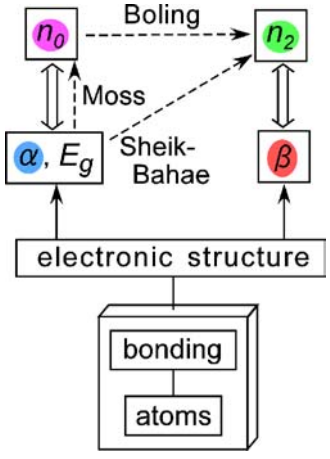

Figure 4 Relationship among atomic structure (atoms and bonding), electronic structure, linear absorption α including bandgap energy E_g, linear refractive index n_0, two-photon absorption β, and nonlinear refractive index n_2. Absorption and refraction are related by linear and nonlinear Kramers-Krőnig relations (double arrows). The Moss rule can be regarded as a simplified Kramers-Krőnig relation. The Bolings' and the Sheik-Bahaes' relation connect n_0 and E_g to n_2, respectively.

Next, $n_0(\omega)$ is expressed using the conventional Kramers-Krőnig relation as [5];

$$n_0(\omega) = 1 + (c/\pi)P \int \{\alpha(\Omega)/(\Omega^2-\omega^2)\}\,\mathrm{d}\Omega. \quad (6)$$

For a nonlinear response Δn, Hutchings *et al.* [47] have derived a relation;

$$\Delta n(\omega;\zeta) = (c/\pi)P \int \{\Delta\alpha(\Omega;\zeta)/(\Omega^2-\omega^2)\}\,\mathrm{d}\Omega, \quad (7)$$

where $\Delta\alpha$ is a nonlinear absorption, which is induced by an excitation at Ω and probed at ζ. Note that this relation is derived rigorously from the causality principle for non-degenerate cases, e.g., two-beam experiments with different photon energies, Ω and ζ. However, this relation may be applied to degenerate cases ($\Omega = \zeta$) as a rough approximation as [46, 48];

$$n_2(\omega) = (c/\pi)P \int \{\beta(\Omega)/(\Omega^2-\omega^2)\}\,\mathrm{d}\Omega. \quad (8)$$

Using these formulas, we can predict gross dependences of β and n_2 upon E_g. Equation 5 suggests $\beta \propto 1/E_g^2$, provided that E_g dependence is governed by $|\Sigma_n 1/(E_{ni}-\hbar\omega)|^2$. This relation may be consistent with the material dependence shown in Fig. 2, which is approximately $\beta_{max} \propto 1/E_g^2$, where β_{max} is a maximal β. Note that this E_g dependence is similar to $\beta \propto 1/E_g^3$, which is theoretically derived and experimentally confirmed for crystalline semiconductors [5, 41]. The difference, E_g^2 and E_g^3, may arise from evaluations of the transition probability. Then, putting $\beta \propto 1/E_g^2$ into Equation 8, and assuming $\int \{1/(\Omega^2-\omega^2)\}\,\mathrm{d}\Omega \propto 1/E_g^2$, we obtain $n_2 \propto 1/E_g^4$, which is consistent with Equation 3. The two rough approximations seem to be cancelled in this $n_2 \sim E_g$ relation. We see that the dependence of n_2 on E_g is much more prominent than that of n_0, i.e., $n_0^4 E_g = 77$. We also can conclude that the large n_2 in chalcogenide glasses is, in essence, due to its small optical gap.

Under some plausible assumptions, we can also calculate the spectral dependence of β and n_2 for an ideal amorphous semiconductor, which contains no gap states [49]. Fig. 5 shows that, at $\hbar\omega = E_g/2$, $\beta = 0$ and n_2 is maximal. This is similar in some degree to the feature at $\hbar\omega = E_g$ for α and n_0. The figure also shows that β becomes maximal at a photon energy between $E_g/2$ and E_g. Note, however, that it is not clear if we can connect this photon-energy dependence with the experimental results shown in Fig. 2, since the observed spectra present much sharper peaks.

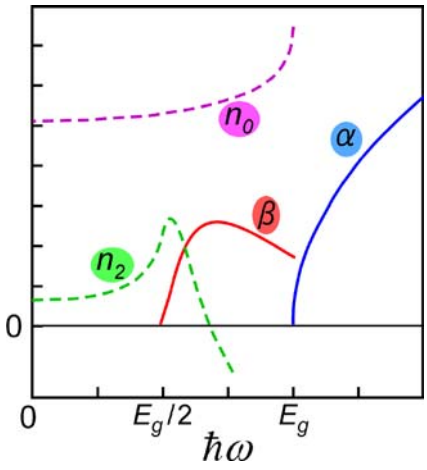

Figure 5 Spectral dependence of linear absorption α, linear refractive-index n_0, two-photon absorption β, and intensity-dependent refractive-index n_2 in an ideal amorphous semiconductor with energy gap E_g [49]. Vertical scales are linear.

2.2.3. Figure of merits

Several figures-of-merit have been proposed for evaluation of optical devices which utilize n_2. For instance, Mizrahi *et al.* [50] and others [9, 26, 51] emphasize unfavorable effects of two-photon absorption, providing a criterion that $2\beta\lambda_0/n_2 < 1$. Then, putting the above E_g dependence, we see $\beta/n_2 \sim E_g^2$, so that small E_g materials would be preferred. Actually, as listed in Table I, in this figure-of-merit, As_2S_3 appears to be better than SiO_2. However, the criterion implicitly neglects the linear absorption α. Lines [20] uses instead n_2/α. Here, α arises from the so-called residual absorption, which is difficult to estimate quantitatively. In addition, not the absorption α, but the attenuation α_0, which includes light scattering, could be decisive. Table I shows that, in this measure, SiO_2 behaves better than As_2S_3. These figures-of-merit however have presumed only non-resonant electronic contributions with sub-ps responses. More recently, Jha *et al.* [15] utilize $n_2/(\tau\alpha)$, where τ is a response time. Nevertheless, theoretical predictions of τ remain to be studied.

Which definition of the figures-of-merit is the most appropriate naturally depends upon the application of interest. For instance, for an optical fiber device, the maximal length could be ~1 m [52], since the device must be compact and fast. Then, the light absorption, which arises from $\alpha + \beta I$, should be suppressed below 10^{-2} cm^{-1}, or light propagation loss must be smaller than ~1 dB/m. However, for optical integrated circuits, an effective propagation distance may be ~1 cm, in which the attenuation could be as large as 10^0 cm^{-1}.

We can suggest another idea by taking the spectrum dependence in Fig. 5 into account. That is, the best material using n_2 at some $\hbar\omega$ is the one which satisfies a bandgap condition of $\hbar\omega = E_g/2$, where α and β are zero and n_2 becomes maximal, provided that there exists no gap-state absorption. In practical glass samples, absorption due to impurities, dangling bonds such as E' centers in oxide glasses [6, 16], and wrong bonds in chalcogenide glasses [6, 49] cannot be neglected. Actually, we see in Fig. 1 and Table I that residual attenuation exists at nominally transparent regions, parts of which are caused undoubtedly by absorption [53]. Note that these mid-gap states also give rise to two-step absorption (see, Fig. 1). We cannot also neglect photoinduced phenomena induced by these photo-electronic excitations (see, Section 5). It is, therefore, not straightforward to select an appropriate glass for some application.

2.3. Stimulated light scattering and super-continuum generation

Recently, stimulated Raman scattering attracts considerable interest, since it provides broad-band light amplification [1, 5]. As illustrated in Fig. 1(d), stimulated Raman scattering can be regarded as a kind of non-degenerate two-photon processes. However, in contrast to the two-photon absorption, in the Raman scattering, one photon is absorbed by virtual states and simultaneously one photon is emitted. When the incident light becomes intense, in a similar way to the conventional stimulated light emission, the Stokes-shifted light could be amplified. Related nonlinear polarization is written down as $P^{(3)}(\omega_s) \propto i\chi_R^{(3)} I(\omega_L)E(\omega_s)$, or emitted light intensity being $\Delta I(\omega_s) \propto \chi_R^{(3)} I(\omega_L)I(\omega_s)$, where ω_L and ω_s ($<\omega_L$) are an exciting laser frequency and a Stokes-shifted frequency.

Most experiments have been done using optical fibers [1, 52] for obtaining long interaction lengths. For instance, as illustrated in Fig. 6, Raman fiber amplifiers with 5–10 km lengths of silica can provide broad-band gains of ~10 dB [54]. Raman lasers using silica microspheres with diameter of ~70 μm [8] are also interesting demonstrations. On the other hand, a few fundamental studies have been reported for stimulated Brillouin scattering [1, 4].

Super-continuum generation in silica fibers and other glasses is now intensively studied [4, 55–58]. When pulsed or cw light propagates through a nonlinear medium, it may undergo spectral broadening [5]. For instance, as illustrated in Fig. 6, a 350-m single-mode fiber, which is excited by a 2.22-W cw laser with a wavelength of 1.483 μm, can emit a 2.1-W output with a broad spectrum extending 1.43–1.53 μm

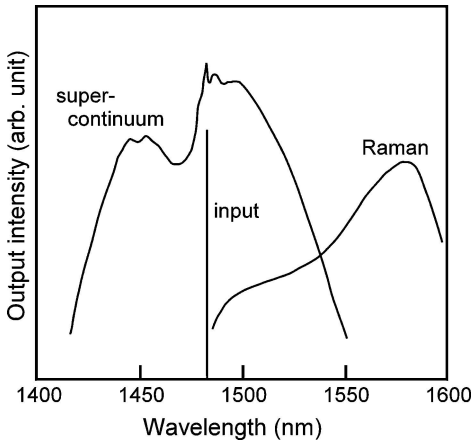

Figure 6 Output spectra of a Raman fiber amplifier [54] and a super-continuum fiber generator [55], which are excited by 1483 nm light (schematic illustration).

[55]. Note that, different from the stimulated light scattering described above, shorter-wavelength light is also generated in this process. The phenomenon appears under strong and prolonged nonlinear interactions, and accordingly, several mechanisms such as intensity-dependent refractive-index changes, third-harmonic generation, and stimulated Raman scattering could be responsible [55]. Such a spectral-conversion fiber could be utilized as a broad-band optical amplifier.

3. Second-order nonlinearity in poled glass

It has been discovered that several kinds of poling methods can add second-order nonlinearity to glasses [13]. At least, five kinds have been demonstrated, which are listed in Table II. Note that similar procedures are employed also for polymers. Most experiments utilize second-harmonic signals for evaluating $\chi^{(2)}$, and less commonly, electro-optical effects. Practical applications remain to be studied, while, for second-harmonic generations, the optical phase matching between exciting and nonlinearly-generated light is a prerequisite [59].

The poling methods can be introduced in the order of discoveries. The so-called optical poling was demonstrated by Österberg and Margulis [14] using optical fibers. They found that an exposure of 70 kW Nd:YAG laser light ($\lambda = 1.06\ \mu$m) for $\sim$1 h to Ge-doped optical fibers with $\sim$1 m length could grow a second-harmonic green signal to 0.55 kW. Stolen and Tom [60] utilized two light beams ($\times$1 and $\times$2 of Nd:YAG laser light) for induction, which could reduce the exposure time to $\sim$5 min. However, the method can apply in practice only to optical fibers, since induced nonlinearity is relatively small, $\chi^{(2)} \approx 10^{-4}$ pm/V. Second, the so-called thermal poling, which was actually electro-thermal, was demonstrated in *bulk* SiO_2 samples by Myers *et al.* [61]. The induced nonlinearity, $\sim$1 pm/V, which was evaluated from second-harmonic signals of 1.06 μm laser light, is a similar magnitude to that in quartz. Since the nonlinearity was considerably large, the method has been applied widely to other oxide [62–64] and chalcogenide [65] glasses. Third, Okada *et al.* [66] demonstrated corona-discharge poling at $\sim$200 °C of 7059 *films* deposited onto Pyrex glass substrates. Such a corona-poling procedure has been commonly employed for organic polymers. Fourth, electron-beam poling of PbO-silica glass could produce $\sim$1 pm/V [67]. An advantage of this method is a high resolution, which may be promising for fabricating optical integrated circuits, despite vacuum is needed. Liu *et al.* [68] applied the method to chalcogenide glasses, producing $\sim$1 pm/V. Proton implantation into silica can also add $\chi^{(2)}$ of $\sim$1 pm/V [69]. Sixth, Fujiwara *et al.* [70] have demonstrated UV-poling in Ge-doped SiO_2 which is subjected to electric fields of $\sim 10^5$ V/cm. The induced $\chi^{(2)}$ is reported to be $\sim$3 pm/V, being comparable to that in $LiNbO_3$.

TABLE II Reported poling methods, applied objects, typical procedure, and induced $\chi^{(2)}$ in silica. References are found in the text. The listed $\chi^{(2)}$ values are compared with $\chi^{(2)}_{11} = 1$ pm/V in crystalline SiO_2 and $\chi^{(2)}_{22} = 5$ pm/V in $LiNbO_3$

Method	Object	Procedure	$\chi^{(2)}$ (pm/V)
Optical	fiber	Nd:YAG laser, 1 h	10^{-4}
Thermal	bulk	4 kV, 300 °C, 1 h	1
Corona	film	5 kV, 300 °C, 15 min	1
e-beam	bulk	40 kV, 10 mA, 10 min	1
Proton	bulk	500 kV, 1 mC, 100 s	1
UV	bulk	ArF laser, 10 kV	3

Two notable poling mechanisms have been proposed [13]. One is that space charges produce a built-in electric field of E_{dc} ($\sim 10^6$ V/cm), which induces effective $\chi^{(2)}$ given as $3E_{dc}\chi^{(3)}$ [60]. Here, E_{dc} is governed by migration of ions such as Na^+ under applied or generated electric fields [71–74]. In consistent with this idea, $\chi^{(2)}$ decays with time constants of 10^1–10^6 days at room temperature, which is connected to alkali ion mobility [74]. The other idea is that oriented defects such as E' centers are responsible. It is reasonable to assume that UV excitation produces defective dipoles, which are oriented along an applied electric field.

It may be reasonable to assume that a dominant mechanism depends upon the poling method. Actually, we can divide the procedures listed in Table II into the two, depending upon whether the glass is heated or unheated during the poling process. The heating tends to enhance macroscopic ion migrations, while simultaneously, it can relax microscopic defect orientations [6]. Therefore, it seems that the ion migration is responsible in the thermal and the corona poling, while the defect orientation is dominant in the other methods. In this context, for enhancing defect orientation, UV poling at low temperatures may be promising.

In so-called *glass ceramics*, embedded crystals seem to be responsible for prominent $\chi^{(2)}$ [64, 65, 75, 76]. For instance, Takahashi *et al.* [76] have demonstrated that oriented $Ba_2TiSi_2O_8$ crystals are produced in BaO-TiO_2-SiO_2 glass by a heat treatment at 760 °C for 1 h, which gives prominent $\chi^{(2)}$ of $\sim$10 pm/V. In such methods, selection of glass composition and how to orient nano-scale crystals are the two key points. $\chi^{(2)}$ can also be generated at interfaces [77].

4. Particle-embedded system

Glasses which contain nano-particles of metals [78, 79] and semiconductors [80] attract considerable interest due to unique third-order nonlinearities. Table III lists several recent results. Such nano-particle dispersed glasses can be prepared by a variety of physical and chemical methods, e.g., vacuum deposition and sol-gel techniques [4, 78, 81]. For semiconductor systems, a lot of work have been done also using semiconductor-doped color glass filters [80], which are commercially available.

These nano-particle systems work efficiently at around resonant wavelengths of some electronic excitations. Such a feature provides, at least, three characteristics. First, not the real, but the imaginary part of $\chi^{(3)}$ could be more prominent. Accordingly, Table III compares the absolute value. Second, the system exhibits strong spectral dependence [4, 88]. For instance,

TABLE III Several particle systems recently reported, with the preparation methods, $|\chi^{(3)}|$, and response time τ at a measured wavelength λ, and references. PLD and VE depict pulsed laser deposition and vacuum evaporation

System	preparation	$\lvert\chi^{(3)}\rvert$ (esu)	τ	λ (nm)	reference
Au (15 nm)/silica	shell structure	10^{-9}	2 ps	550	82
Cu (2 nm)/Al_2O_3	PLD	10^{-7}	5–450 ps	600	83
Ag (20 nm)/BaO	VE	10^{-10}	0.2 ps	820	84
Fe (4 nm)/$BaTiO_3$	PLD	10^{-6}		532	85
SnO_2(10 nm)/silica	sol-gel	10^{-12}		1064	86
CdS (4 nm)/silica	sol-gel	10^{-11}		500	87

Au-silica and CdSSe-silica are efficient at ~580 nm and ~800 nm [4]. Third, the response time τ and the linear absorption α tend to become longer and higher. Actually, a trade-off between $\chi^{(3)}$ and the two, τ and α, seems to exist. For instance, CdSSe-dispersed glasses show $\chi^{(3)} \approx 10^{-9}$ esu with $\tau \approx 20$ ps, while in Au-dispersed glasses $\sim 10^{-11}$ esu and ~1 ps [4]. Linear absorption could be as large as 10^4 cm^{-1} [78], so that these systems can be utilized as small devices, not as fibers. Note that, in pure silica at non-resonant infrared wavelength, $\chi^{(3)} \approx 10^{-13}$ esu, $\tau \approx 10$ fs, and $\alpha \leq 10^{-5}$ cm^{-1} [78].

As is suggested above, the particle-embedded system should surmount two problems for wide applications. One is the reduction of linear attenuation, including absorption and scattering, and the other is the shift of resonant wavelengths to the optical communication region, 1.3–1.5 μm. Is such a shift possible? What are the mechanisms giving rise to the prominent nonlinearity?

When the particle is a semiconductor such as CuCl and CdSSe, excitons or confined electron-hole pairs are responsible [80]. Specifically, the exciton in semiconductor particles can be treated as a two-level system, and at the resonance frequency, $|\chi^{(3)}|$ is written as;

$$\left|\chi^{(3)}\right| \approx \mathrm{Im}\,\chi^{(3)} \propto |\mu|^4 N T_1 T_2^2, \tag{9}$$

where μ is the dipole moment of excitons, N the particle number, T_1 (≈100 ps) the life time of excitons, T_2 (≈fs) the dephasing time. A quantitative estimation predicts that a closely-packed CuCl particles with radius of 40 nm could provide a $|\chi^{(3)}|$ enhancement of a factor of $\sim 10^3$ when compared with the bulk value [89]. Nevertheless, the close-packing of such particles without inter-particle interaction may not be easily attained.

When the particle is metals such as spherical Au with diameters of 10–50 nm, we can envisage local field enhancement and dynamic responses of conduction electrons including plasmon effects [78, 79]. The result is approximately written as [90];

$$\chi^{(3)} \approx p_\mathrm{m} \chi_\mathrm{m}^{(3)} |3\varepsilon_\mathrm{h}/(\varepsilon_\mathrm{m} + 2\varepsilon_\mathrm{h})|^2 \{3\varepsilon_\mathrm{h}/(\varepsilon_\mathrm{m} + 2\varepsilon_\mathrm{h})\}^2, \tag{10}$$

where p_m is the volume fraction of metal particles, $\chi_\mathrm{m}^{(3)}$ the bulk nonlinearity of the metal, and ε_h and ε_m the linear dielectric constants of host (glass) and the metal. Nonlinearity of the host is neglected for simplicity here. Note that ε_h may be real, while ε_m is complex. We see in this expression that the metal nonlinearity $\chi_\mathrm{m}^{(3)}$ is decreased by the volume factor p_m, while $\chi_\mathrm{m}^{(3)}$ may be enhanced by local fields if $\mathrm{Re}(\varepsilon_\mathrm{m} + 2\varepsilon_\mathrm{h}) \approx 0$, which determines the resonance wavelength. In consistent with this model, an Au-dispersed glass, for instance, gives a greater $\chi^{(3)}$ than that of Au films [5].

However, since these systems are complex consisting of particles and a glass matrix, a variety of situations arise. For the particle, we should consider, in addition to particle species, size, size distribution, shape, and concentration [91]. Here, needlessly, a narrow size distribution is preferred for investigating fundamental mechanisms. The shape may be spherical, ellipsoidal, rod, and so forth [92]. The concentration determines a mean separation distance between particles. With concentration increases, particle-particle electric interaction appears [82], and then the particles eventually percolate [83], which may give dramatic changes in nonlinear responses. On the other hand, the matrix seems to provide secondary importance. Actually, not only glasses but also liquids and organic materials have been employed [4]. However, some reports suggest that the nonlinearity is largely affected by surface states of semiconductor particles [93] and by dielectric constants of matrix surrounding metallic particles [4].

Lastly, it may be worth mentioning two pioneering studies. One is that particles can be arrayed to produce photonic structures, which exhibit novel nonlinear properties such as light confinement [94]. The other is generation of second-harmonic signals from oriented ellipsoidal Ag nano-particles [95]. The oriented-particle structure has been produced in silica through tensile deformation and simultaneous heating, which may be regarded as a kind of mechanical poling.

5. Photoinduced phenomena

Intense pulsed light, which is employed for producing nonlinear effects, is likely to provide also a variety of transitory and (quasi-)stable optical changes [93, 96]. Photochromic effects induced by sub-gap light may be known as transitory electronic changes [97]. The refractive-index increase [16,98–101] and structural modifications [102] in SiO_2 and other glasses induced by fs–ns laser light with $\hbar\omega \approx 1 \sim 5$ eV is known to arise from quasi-stable structural changes. Optical poling described in Section 3 can be regarded as a kind of photoinduced anisotropy [103]. When light is more intense than 1 GW/cm^2–1 TW/cm^2, which varies with the duration of light pulses, permanent damages are likely to occur [5, 104]. These varieties of changes are induced by electronic excitations, which may be

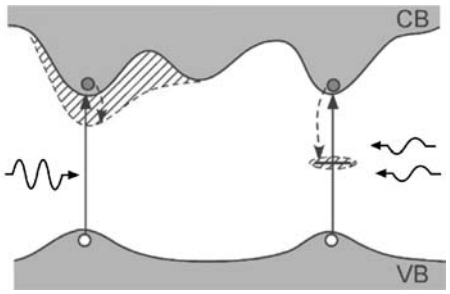

Figure 7 Different relaxation paths induced by bandgap excitation provided by one-photon (left) and two-photon (right) processes. For instance, the one-photon and two-photon excitations may induce bonding strains and defect alterations.

triggered by one-photon and multi-photon processes, depending upon photon energy and light intensity. After such photoelectronic excitation, electro-structural or electro-thermal processes may follow.

Are these photoinduced phenomena really excited by nonlinear excitation? For instance, it is often asserted that, when some photoinduced phenomenon is induced by exposures to light with photon energy of $\hbar\omega \approx E_g/m$, where m is an integer, m-photon absorption is responsible [105, 106]. Nevertheless, the phenomenon may be excited by one-photon absorption by mid-gap states, which give weak absorption tails (see, Fig. 2) arising from defective structures in glasses [6, 101]. Otherwise, it may be excited by m-step absorption processes [107], consisting of successive m-times one-photon absorption (see, Fig. 1(c)). These processes have probably been overlooked when analyzing experimental results.

In addition, as schematically illustrated in Fig. 7, structural changes induced by linear and nonlinear excitation cannot necessarily be the same. Tanaka has demonstrated using As_2S_3 that bandgap excitations produced by one-photon and by two-photon absorption provide different changes [101]. The one-photon excitation gives photodarkening, while the two-photon gives refractive-index increase with *no* photodarkening. In these phenomena, temperature rises by intense exposures can be neglected.

Such changes depending upon excitation processes can appear in glasses. This is because the *localized* atomic wavefunction plays important roles, the situation which is contrastive to extended Bloch wavefunctions in crystals. For instance, as we see in Equation 4, that the one-photon excitation occurs between wavefunctions having different parities, such as from s to p-orbital, since H is an odd function. In contrast, Equation 5 shows that the two-photon excitation can occur between the same-parity states, such as from p to p. In addition, $1/(E_{ni} - \hbar\omega)$ in the equation gives a possibility of *resonant and localized* two-photon excitation if $E_{ni} - \hbar\omega \approx 0$ is satisfied for some mid-gap state. In such cases, the mid-gap state selectively absorbs the excitation energy, leading to some localized atomic change around the state. If the change is densely accumulated, it will appear as a macroscopic photoinduced phenomenon. Situations occurring in glasses are not so simple as those in single crystals.

6. Summary

We, at present, have a big gap between science and technology of glasses. In a physical point-of-view, the glass science remains to be far behind of the crystal science, the main reasons being due to experimental difficulty in atomic-structure determination and theoretical unavailability of Bloch-type wavefunctions. On the contrary, we cannot imagine any more a world without photonic glasses such as optical fibers. These contrastive science-technology situations require and promote deeper understandings and wider applications of nonlinear photonic glasses.

The third-order optical nonlinearity in homogeneous glasses has been studied in some details. Substantial experimental data are available for n_2, which have been analyzed using empirical relations such as Bolings'. In contrast, less work has been done for nonlinear absorption β. In the present article, therefore, we have tried to understand in a coherent way the absorption and the refractive index using semiconductor terminology. The approach can connect these nonlinear properties to the energy gap. However, little work has been done for dynamics. For instance, it is difficult to theoretically predict the response time τ in a glass at some excitation energy.

Two inhomogeneous systems arouse growing interests. One is the poled or crystallized glass. Greater second-order nonlinearity has been reported, some of which can be added to selected regions. The other is the particle-embedded system, which can provide greater third-order, and in some cases, second-order nonlinearity. However, the mechanism remains to be studied. An experimental problem is the method which can reproduce fixed-size and -shape particles with arbitrary concentration. These two inhomogeneous systems can be combined with photonic-structure concepts, which will be interesting for future applications.

Finally, in a variety of photoinduced phenomena in glasses, nonlinear optical excitations appear to play some important roles. However, fundamental studies are still lacking. The phenomenon may just seemingly be nonlinear, and alternatively, linear excitation of gap states could trigger successive changes. Understandings of the nonlinear photo-electro-structural process will be challenging problems.

Appendix: Defining terms

Abbe number: A number ν_d which is a measure of the dispersion (wavelength-dependence) of refractive index n of transparent materials at visible wavelengths. $\nu_d = (n_d - 1)/(n_F - n_C)$, where $d = 587$ nm, $F = 486$ nm, and $C = 656$ nm. ν_d takes values of 80 - 20, which decreases with increasing n_d from 1.5 to 1.9.

All-optical switch: Optical inputs are switched by other optical signals. The switching is produced in many cases by refractive-index changes. Comparing electronic devices such as transistors, in which an electrical input is controlled by an electrical current, we expect that the all-optical switch can work faster, being free from electrical noises. However, at present, in

contrast to the μm scale of a transistor, an all-optical switch may have cm scales.

Centro-symmetric: A crystal structure in which a center of inversion exists is called as centro-symmetric. There are 32 crystal classes, among which 11 are centro-symmetric.

Corona discharge: When a high voltage of 5–10 kV is applied to sharp edges or fine wires of metals, the gas such as air surrounding the metal is ionized and discharged. If the voltage is dc, ions having the same polarity with the dc voltage move toward a grounded electrode.

Dangling bond: A kind of point-like defects which is produced by breaking covalent bonds. The dangling bond may have an unpaired electron, paired two electrons, or no electrons. These dangling bonds were denoted as D^0, D^-, and D^+ by Mott, the superscript representing the charge state.

E' center: A kind of unpaired-electron dangling bonds in oxide glasses. In SiO_2, an Si atom which is bonded to three O atoms may have one E' center. The center, which may be produced by radiation, gives ESR signals and optical absorption at $\hbar\omega \approx 6$ eV.

Exciton: An electron-hole pair, which behaves as a H atom, with binding energy of 10–100 meV and life time of $\sim$1 ns. The wavefunction, in principle, extends over the whole crystal.

Miller's rule: An empirical rule proposed by Miller in 1964, which suggests that $\chi^{(2)}/\{\chi^{(1)}\}^3$ is nearly constant for all non-centrosymmetric crystals.

Photochromic: Temporal coloring induced by (UV) light illumination. For instance, photo-structural changes of Ag particles, which are dispersed in oxide glasses, are responsible.

Photodarkening: Quasi-stable darkening induced by light illumination. In chalcogenide glasses, it occurs with a red-shift of optical absorption edge, which is induced through athermal photo-structural processes. The process, however, is speculative.

Photonic glass: High-purity glasses in which impurities are controlled or suppressed at ppm levels. An example is the optical fiber glass developed at the end of 20 century, which is very recent when compared to a long history of artificial glasses for 5000 years.

Plasmon: Quantized collective motions of electron gas in a metal. In a bulk metal, the plasmon propagates as a longitudinal wave, which may be probed by an electron beam. In a metal nano-particle, a transversal surface plasmon can be excited by light waves.

Power stabilizer: An optical device which can provide a fixed output intensity upon varying input intensity. The principle may be based on multi-photon absorption, which becomes efficient when light is more intense.

Short-range atomic structure: Atomic bonding structures within a scale of $\sim$0.5 nm, which are characterized by coordination number (the number of nearest neighbor atoms), bond length, and bond angle. It is demonstrated for such simple glasses as SiO_2 that the short-range structure is nearly the same with that in a corresponding crystal.

Tauc gap: Tauc discovered that, in many chalcogenide glasses such as As_2S_3, optical absorption spectra α around the fundamental edge can be fitted as $\alpha\hbar\omega \propto (\hbar\omega - E_g)^2$, where E_g is called as Tauc gap. The energy is often used as a measure of optical bandgap, while its theoretical interpretation is not conclusive.

Two-step absorption: A successive one-photon absorption via a gap state (Fig. 1(c)). Since the gap state has some cross section, the absorption is assumed to occur as functions of light intensity and pulse duration as well.

Wrong bond: Homopolar bonds in stoichiometric glasses, such as As-As in As_2S_3. The defective bond nominally does not exist in the corresponding crystal. However, specifically in covalent glasses such as As_2S_3, the bond exists with a concentration of $\sim$1%, which depends upon preparation methods and so forth.

Acknowledgments

The author would like to thank his students, K. Sugawara and N. Minamikawa, for preparing illustrations and giving comments.

References

1. G. P. AGRAWAL, "Nonlinear Fiber Optics" 3rd Ed. (Academic Press, San Diego, 2001).
2. P. P. MITRA and J. B. STARK, *Nature* **441** (2001)1027.
3. L. F. MOLLENAUER, *Science* **302** (2003) 996.
4. R. L. SUTHERLAND, "Handbook of Nonlinear Optics" 2nd Ed. (Marcel Dekker, New York, 2003).
5. R. W. BOYD, "Nonlinear Optics" 2nd Ed. (Academic Press, San Diego, 2003).
6. S. R. ELLIOTT, "Physics of Amorphous Materials" 2nd Ed., (Longman Scientific & Technical, Essex, 1990).
7. M. H. FIELD, J. POPP and R. K. CHANG, "Progress in Optics" Edited by E. Wolf (North Holland, Amsterdam, 2000), Vol. 41, Chap. 1.
8. S. M. SPILLANE, T. J. KIPPENBERG and K. J. VAHALA, *Nature* **415** (2002) 621.
9. A. ZAKERY and S. R. ELLIOTT, *J. Non-Cryst. Solids* **330** (2003) 1.
10. H. EBENDORFF-HEIDEPRIEM, P. PETROPOULOS, R. MOORE, K. FRAMPTON, D. J. RICHARDSON and T. M. MONRO, *ibid.* **345/346** (2004) 293.
11. A. K. MAIRAJ, R. J. CURRY and D. W. HEWAK, *Appl. Phys. Lett.* **86** (2005) 94102.
12. S. E. SKIPETROV, *Nature* **432** (2004) 285.
13. Y. QUIQUEMPOIS, P. NIAY, M. DOUNAY and B. POUMELLEC, *Curr. Opinion Sol. St. Mater. Sci.* **7** (2003) 2003.
14. U. OSTERBERG and W. MARGULIS, *Opt. Lett.* **11** (1986) 516.
15. A. JHA, X. LIU, A. K. KAR and H. T. BOOKEY, *Curr. Opinion Sol. St. Mater. Sci.* **5** (2001) 475.
16. G. PACCHIONI, L. SKUJA and D. L. GRISCOM, "Defects in SiO_2 and Related Dielectrics: Science and Technology" (Kluwer, Dortrecht, 2000).
17. E. M. VOGEL, M. J. WEBER and D. M. KROL, *Phys. Chem. Glasses* **32** (1991) 231.
18. Y. CHENG, K. SUGIOKA and K. MIDORIKAWA, *Opt. Lett.* **29** (2004) 2007.
19. Y. IGA, T. ISHIZUKA, W. WATANABE, K. ITOH, Y. LI and J. NISHII, *Jpn. J. Appl. Phys.* **43** (2004) 4207.
20. M. E. LINES, *J. Appl. Phys.* **69** (1991) 6876.

21. R. E. SLUSHER, G. LENZ, J. HODELIN, J. SANGHERA, L. B. SHAW and I. D. AGGARWAL, *J. Opt. Soc. Am.* **B21** (2004) 1146.
22. E. L. FALCAO, C. B. DE ARAUJO, C. A. C. BOSCO, G. S. MACIEL, L. H. ACIOLI, M. NALIN and Y. MASSADEP, *J. Appl. Phys.* **97** (2005) 13505.
23. J. M. LANIEL, N. HO, R. VALLEE and A. VILLENEUVE, *J. Opt. Soc. Am.* **B22** (2005) 437.
24. J. T. GOPINATH, M. SOLJACIC, E. P. IPPEN, V. N. FUFLYIGIN, W. A. KING and M. SHURGALIN, *J. Appl. Phys.* **96** (2004) 6931.
25. A. ZARKEY and M. HATAMI, *J. Opt. Soc. Am.* **B22** (2005) 591.
26. K. OGUSU, J. YAMASAKI, S. MAEDA, M. KITAO and M. MINAKATA, *Opt. Lett.* **29** (2004) 265.
27. Y. IMAI and K. MIZUTA, *ibid.* **25** (2000) 1412.
28. K. TANAKA, *J. Non-Cryst. Solids* **338–340** (2004) 534.
29. K. IMANISHI, Y. WATANABE, T. WATANABE and T. TSUCHIYA, *J. Non-Cryst. Solids* **259** (1999) 139.
30. K. TANAKA, N. YAMADA and M. OTO, *Appl. Phys. Lett.* **83** (2003) 3012.
31. K. TANAKA, *ibid.* **80** (2002) 177.
32. K. TANAKA, *J. Opteletro. Adv. Mater.* **4** (2002) 505.
33. R. C. ENCK, *Phys. Rev. Lett.* **31** (1973) 220.
34. P. S. WEITZMAN and U. OSTERBERG, *J. Appl. Phys.* **79** (1996) 8648.
35. T. MIZUNAMI and K. TAKAGI, *Opt. Lett.* **19** (1994) 463.
36. A. DRAGONMIR, J. G. MCLNERNEY and N. NIKOGOSYAN, *Appl. Opt.* **41** (2002) 4365.
37. N. L. BOLING, A. J. GLASS and A. OWYOUNG, *IEEE Quant. Electro.* **QE-14** (1978) 601.
38. V. DIMITROV and S. SAKKA, *J. Appl. Phys.* **79** (1996) 1741.
39. J. QI, D. F. XUE and G. L. NING, *Phys. Chem. Glasses* **45** (2004) 362.
40. S. SUEHARA, P. THOMAS, A. MIRGORODSKY, T. MERLE-MEJEAN, J. C. CHAMPARNAUD-MESJARD, T. AIZAWA, S. HISHITA, S. TODOROKI, T. KONISHI and S. INOUE, *J. Non-Cryst. Solids* **345/346** (2004) 730.
41. M. SHEIK-BAHAE, D. J. HAGAN and E. W. VAN STRYLAND, *Phys. Rev. Lett*. **65** (1990) 96.
42. T. S. MOSS, "Optical Properties of Semi-conductors" (Butterworths Sci. Pub., London, 1959) p. 48.
43. N. SUGIMOTO, H. KANBARA, S. FUJIWARA, K. TANAKA and K. HIRAO, *Opt. Lett.* **21** (1996) 1637.
44. S. SMOLORZ, I. KANG, F. WISE, B. G. AIKEN and N. F. BORRELLI, *J. Non-Cryst. Solids* **256/257** (1999) 310.
45. O. SUGIMOTO, H. NASU, J. MATSUOKA and K. KAMIYA, *ibid.* **161** (1993) 118.
46. K. TANAKA and N. MINAMIKAWA, *Appl. Phys. Lett.* **86** (2005) 121112.
47. D. C. HUTCHINGS, M. SHEIK-BAHAE, D. J. HAGAN and E. W. VAN STRYLAND, *Opt. Quantum Electron.* **24** (1992) 1.
48. M. SHEIK-BAHAE, D. C. HUTCHINGS, D. J. HAGAN and E. W. VAN STRYLAND, *IEEE Quant. Electron.* **QE-27** (1991) 1296.
49. K. TANAKA, "Optoelectronic Materials and Devices" Edited by G. Lucovsky and M.Popescu (INOE Publishing House, Bucharest, 2004) Vol. 1, Ch. 3.
50. V. MIZRAHI, K. W. DELONG, G. I. STEGEMAN, M. A. SAIFI and M. J. ANDREJCO, *Opt. Lett.* **14** (1989) 1140.
51. M. ASOBE, *Opt. Fiber Technol.* **3** (1997) 142.
52. G. I. STEGEMAN and R. H. STOLEN, *J. Opt. Soc. Am. B* **6** (1989) 652.
53. K. TANAKA, T. GOTOH, N. YOSHIDA and S. NONOMURA, *J. Appl. Phys.* **91** (2002) 125.
54. J. BROMAGE, *J. Lightwave Technol.* **22** (2004) 79.
55. A. ZHELTIKOV, *Appl. Phys. B: Lasers and Optics* **77** (2003) 143.
56. A. K. ABEELUCK and C. HEADLEY, *Appl. Phys. Lett.* **85** (2004) 4863.
57. Y. NI, Q. WANG, X. LIU, J. PENG and B. ZHOU, *ibid.* **85** (2004) 3384.
58. X. H. NI, C. WANG, X. C. LIANG, M. AL-RUBAIEE, R. R. ALFANO, *IEEE J. Selected Topics Quant. Electro.* **10** (2004) 1229.
59. H.-Y. CHEN, C.-L. LIN, Y.-H. YANG. S. CHAO, H. NIU and C. T. SHIH, *Appl. Phys. Lett.* **86** (2005) 81107.
60. R. H. STOLEN and H. W. K. TOM, *Opt. Lett.* **12** (1987) 585.
61. R. A. MYERS, N. MUKHERJEE and S. R. J. BRUECK, *ibid.* **22** (1991) 1732.
62. Y. LUO, A. BISWAS, A. FRAUENGLASS and S. R. BRUECK, *Appl. Phys. Lett.* **84** (2004) 4935.
63. B. FERREIRA, E. FARGIN, J. P. MANAUD, G. LE FLEM, V. RODRIGUEZ and T. BUFFETEAU, *J. Non-Cryst. Solids* **343** (2004) 121.
64. G. S. MURUGAN, T. SUZUKI, Y. OHISHI, Y. TAKAHASHI, Y. BENINO, T. FUJIWARA and T. KOMATSU, *Appl. Phys. Lett.* **85** (2004) 3405.
65. M. GUIGNARD, V. NAZABAL, J. TROLES, F. SMEKTALA, H. ZEGHLACHE, Y. QUIQUEMPOIS, A. KUDLINSKI and G. MARTINELLI, *Opt. Exp.* **13** (2005) 789.
66. A. OKADA, K. ISHII, K. MITO and K. SASAKI, *Appl. Phys. Lett.* **60** (1992) 2853.
67. P. G. KAZANSKY, A. KAMAL and P.ST. RUSSELL, *Opt. Lett.* **18** (1993) 683.
68. Q. M. LIU, F. X. GAN, X. J. ZHAO, K. TANAKA, A. NARAZAKI and K. HIRAO, *ibid.* **26** (2001) 1347.
69. L. J. HENRY, B. V. MCGRATH, T. G. ALLEY and J. J. KESTER, *J. Opt. Soc. Am. B* **13** (1996) 827.
70. T. FUJIWARA, M. TAKAHASHI and A. J. IKUSHIMA, *Appl. Phys. Lett.* **71** (1997) 1032.
71. H. L. AN, S. FLEMING and G. COX, *Appl. Phys. Lett.* **85** (2004) 5819.
72. V. TREANTON, N. GODBOUT and S. LACROIX, *J. Opt. Soc. Am.* **B21** (2004) 2213.
73. Y. QUIQUEMPOIS, A. KUDLINSKI and G. MARTINELL, *J. Opt. Soc. Am.* **B22** (2005) 598.
74. O. DEPARIS, C. CORBARI, G. KAZANSKY and K. SAKAGUCHI, *Appl. Phys. Lett.* **84** (2004) 4857.
75. V. PRUNERI, P. G. KAZANSKY, D. HEWAK, J. WANG, H. TAKEBE and D. N. PAYNE, *Appl. Phys. Lett.* **70** (1997) 155.
76. Y. TAKAHASHI, K. KITAMURA, Y. BENINO, T. FUJIWARA and T. KOMATSU, *ibid.* **86** (2005) 91110.
77. R. T. HART, K. M. OK, P. S. HALASYAMANI and J. W. ZWANZIGER, *ibid.* **85** (2004) 938.
78. F. GONELLA and P. MAZZOLDI, "Handbook of Nanostructured Materials and Nanotechnology" edited by H.S. Nalwa (Academic Press, San Diego, 2000) Vol. 4, Chap. 2.
79. V. M. SHALAEV, "Nonlinear Optics of Random Media" (Springer, Berlin, 2000).
80. G. BANFI, V. DEGIORGIO and D. RICARD, *Adv. Phys.* **47** (1998) 510.
81. M. NOGAMI, S. T. SELVAN and H. SONG, "Photonic Glasses: Nonlinear Optical and Spectral Hole Buring Properties" in *Handbook of Advanced Electronic and Photonic Materials and Devices*, H.S. Nalwa edited by (Academic Press, San Diego, 2001) Vol. 5, Chapter 5.
82. Y. HAMANAKA, K. FUKUTA, A. NAKAMURA, L. M. LIZ-MARZAN and P. MULVANEY, *Appl. Phys. Lett.* **84** (2004) 4938.
83. R. DEL COSO, J. REQUEJO-ISIDRO, J. SOLIS, J. GONZALO and C. N. AFONSO, *J. Appl. Phys.* **95** (2004) 2755.
84. Q. F. ZHANG, W. M. LIU, Z. Q. XUE, J. L. WU, S. F. WANG, D. L. WANG and Q. H. GONG, *Appl. Phys. Lett.* **82** (2003) 958.
85. W. WANG, G. YANG, Z. CHEN, Y. ZHOU, H. LU and G. YANG, *J. Appl. Phys.* **92** (2002) 7242.
86. A. CLEMENTI, N. CHIODINI and A. PALEARI, *Appl. Phys. Lett.* **84** (2004) 960.
87. S. G. LU, Y. J. YU, C. L. MAK, K. H. WONG, L. Y. ZHANG and X. YAO, *Microelectronic Eng.* **66** (2003) 171.
88. J. HE, W. JI, G. H. MA, S. H. TANG, H. I. ELIM, W. X. SUN, Z. H. ZHANG and W. S. CHIN, *J. Appl. Phys.* **95** (2004) 6381.

89. Y. LI, M. TAKATA and A. NAKAMURA, *Phys. Rev. B* **57** (1998) 9193.
90. D. STROUD and P. M. HUI, *ibid.* **37** (1988) 8719.
91. P. D. PERSANS, T. M. HAYES and L. B. LURIO, *J. Non-Cryst. Solids* **349** (2004) 315.
92. J. L. GU, J. L. SHI, G. J. YOU, L. M. XIONG, S. X. QIAN, Z. L. HUA and H. R. CHEN, *Adv. Mater.* **17** (2005) 557.
93. A. PUZDER, A. J. WILLIAMSON, F. GYGI and G. GALLI, *Phys. Rev. Lett.* **92** (2004) 217401.
94. M. AJGAONKAR, Y. ZHANG, H. GREBEL and C. W. WHITE, *Appl. Phys. Lett.* **75** (1999) 1532.
95. A. PODLIPENSKY, J. LANGE, G. SEIFERT, H. GRAENER and I. CRAVETCHI, *Opt. Lett.* **28** (2003) 716.
96. R. C. JIN, Y. C. CAO, E. C. HAO, G. S. METRAUX, G. C. SCHATZ and C. A. MIRKIN, *Nature* **425** (2003) 487.
97. Y. WATANABE, Y. KIKUCHI, K. IMANISHI and T. TSUCHIYA, *Mater. Sci. Eng.* **B54** (1998) 11.
98. A. SALIMINIA, N. T. NGUYEN, M.-C. NADEAU, S. PETIT, S. L. CHIN and R. VALLEE, *Appl. Phys. Lett.* **93** (2003) 3724.
99. S. J. MIHAILOV, C. W. SMELSER, D. GROBNIC, R. B. WALKER, P. LU, H. DING and J. UNRUH, *J. Lightwave Technol.* **22** (2004) 94.
100. J. SIEGEL, J. M. FERNANDEZ-NAVARRO, A. GARCIA-NAVARROR, V. DIEZ-BLANCO, O. SANZ, J. SOLIS, F. VEGA and J. ARMENGOL, *Appl. Phys. Lett.* **86** (2005) 121109.
101. K. TANAKA, *Philos. Mag. Lett.* **84** (2004) 601.
102. Y. SHIMOTSUMA, P. G. KAZANSKY, J. R. QIU and K. HIRAO, *Phys. Rev. Lett.* **91** (2003) 247405.
103. C. CORBARI, P. G. KAZANSKY, S. A. SLATTERY and D. N. NIKOGOSYAN, *Appl. Phys. Lett.* **86** (2005) 71106.
104. N. T. NGUYEN, A. SALIMINIA, W. LIN, S. L. CHIN and R. VALLEE, *Opt. Lett.* **28** (2003) 1591.
105. A. ZOUBIR, M. RICHARDSON, C. RIVERO, A. SCHULTE, C. LOPEZ, K. RICHARDSON, N. HO and R. VALLEE, *ibid.* **29** (2004) 748.
106. G. BOUDEBS, S. CHERUKULAPPURATH, M. GUIGNARD, J. TROLES, F. SMEKTALA, and F. SANCHEZ, *Opt. Commun.* **232** (2004) 417.
107. K. KAJIHARA, Y. IKUTA, M. HIRANO and H. HOSONO, *Appl. Phys. Lett.* **81** (2002) 3164.

Received 19 December 2004
and accepted 19 April 2005